

*This study examines the effect of a hydrated lime additive on steel slag stone mastic asphalt for induction heating and induced healing applications. It evaluates the self-healing capabilities of hydrated lime-modified steel slag stone mastic asphalt under tropical conditions.*

*The three-point bending was first tested on the steel slag-stone mastic asphalt mixture modified with hydrated lime (1 %, 2 %, 3 %, and 4 % by mix weight). The mix's fracture, displacement, cracking resistance, and flexibility index are evaluated. Subsequently, the fracture, displacement, cracking resistance, flexibility index recovery, and healing ratio for damage-healing were investigated. The research employs induction heating, which regulates temperature according to natural tropical conditions. The healing process is compared between heating in a tropical environment and heating with additional temperature.*

*The results demonstrated that adding hydrated lime to steel slag stone mastic asphalt increased fracture strength, however, this improvement was accompanied by decreased displacement, cracking resistance, and flexibility. The findings indicate that the healing ratio of steel slag stone mastic asphalt is enhanced by 1 % hydrated lime. Adding 1 % hydrated lime is optimal for improving fracture strength and healing ratio. The fracture strength increased by 5 % with a 1 % variation of hydrated lime. The healing ratio of the 1 % hydrated lime-modified stone mastic asphalt increased by 14.57 % under natural conditions compared to 0 % hydrated lime steel slag stone mastic asphalt. Furthermore, the healing ratio of steel slag mastic asphalt with 1 % hydrated lime subjected to artificial heating increased by 22.08 % compared to stone mastic asphalt with 0 % hydrated lime under natural heating*

**Keywords:** steel slag, stone mastic asphalt, heating induction, self-healing, three-point bending test, tropical condition

# IDENTIFYING THE EFFECT OF THE HYDRATED LIME ON SELF-HEALING STEEL SLAG STONE MASTIC ASPHALT USING THE INDUCTION HEATING METHOD IN TROPICAL CONDITIONS

**Irawati**

Assistant Professor of Civil Engineering\*

**Ludfi Djakfar**

Corresponding author

Professor of Civil Engineering\*\*

E-mail: ldjakfar@ub.ac.id

**Muhammad Zainul Arifin**

Associate Professor of Civil Engineering\*\*

**Akhmad Sabarudin**

Professor of Material and Analytical Chemistry\*\*

**Ilanka Cahya Dewi**

Assistant Professor of Civil Engineering\*

**Irawan Palgunadi**

Manager Research & Development

Krakatau Steel Indonesia Company

Industri str., 5, Cilegon Banten, West Java, Indonesia, 42435

\*Department of Civil Engineering

Universitas Muhammadiyah Jember

Karimata str., 49, Jember, East Java, Indonesia, 68121

\*\*Department of Civil Engineering

Universitas Brawijaya

Veteran str., 10-11, Malang, East Java, Indonesia, 65145

Received 03.02.2025

Received in revised form 31.03.2025

Accepted date 16.04.2025

Published date 30.04.2025

**How to Cite:** Irawati, I., Djakfar, L., Arifin, M. Z., Sabarudin, A., Dewi, I. C., Palgunadi, I. (2025). Identifying the effect of the hydrated lime on self-healing steel slag stone mastic asphalt using the induction heating method in tropical conditions. *Eastern-European Journal of Enterprise Technologies*, 2 (6 (134)), 33–43.  
<https://doi.org/10.15587/1729-4061.2025.325722>

## 1. Introduction

Steel slag stone mastic asphalt is a composite mixture of high-quality crushed stone, steel slag, fine aggregates, asphalt binder, a significant percentage of mineral filler, and cellulose to prevent draindown. Incorporating steel slag with stone mastic asphalt enhances concrete asphalt mixtures' durability and self-healing capacity. Adding hydrated lime to steel stone mastic asphalt enhances adhesion, affecting stability and water resistance. However, incorporating hydrated lime (HL) into the mixture necessitates a review of self-healing capacity, fracture resistance, and crack resistance, as adding HL to asphalt mastic increases stiffness and reduces strain tolerance. Self-healing through induction heating lowers the viscosity of the asphalt in the mixture, allowing the asphalt to fill cracks due to gravity, surface tensile stress, and pressure caused by temperature. In other words, the self-healing induction heating method is sensitive to changes

in viscosity and temperature, which contrasts with the HL effect that tends to increase viscosity. Thus, it is crucial to establish an optimal dosage where increased stiffness does not compromise self-healing capacity.

HL on mastic asphalt has also shown performance dependence on HL concentration, with the test temperatures. Thus, modifying hydrated lime in steel slag stone mastic asphalt must be tested against the self-healing capacity under heating conditions. In tropical climates, asphalt pavement's self-healing ability requires minimal effort to increase its surface temperature and reduce its viscosity, which holds great potential for applying self-healing technology.

To apply self-healing technology, it is necessary to test the impact of hydrated lime on self-healing performance under tropical conditions. Self-healing ability is beneficial for improving the quality of the road. Stability, durability, water resistance, and self-healing ability are a great combination to increase the service life of the road. Therefore, the self-heal-

ing ability of modified stone mastic asphalt with steel slag and hydrated lime is scientifically relevant to investigate.

## 2. Literature review and problem statement

Hydrated lime (HL) has been recognized as an additive for asphalt mixture and has attracted significant interest. HL strongly influences the durability of asphalt mixtures [1, 2]. It enhances adhesion between the asphalt binder and aggregates, reduces fatigue damage rates, and increases the service life of asphalt pavements. However, the study only tested the impact of HL on asphalt mastic, which was not in the form of an asphalt concrete mixture. Thus, it is still necessary to test whether asphalt mastic with HL incorporates steel slag stone mastic asphalt (SMASS).

Using HL in stone mastic asphalt (SMA) mixtures demonstrates the potential benefits of HL as a filler that optimizes the cracking performance and durability under varying temperatures [3]. The experimental results show a significant dependence between the HL concentration and the test temperature. The increase in stability is reasonable because stone mastic asphalt is a hot mix asphalt with an extensive void range of 3–6 % of the volume of the mix. As an additive or as a filler substitution, HL enhances the function of filling a void, increasing rigidity, adhesion, stability, and water resistance.

Previous research has proven that incorporating steel slag with stone mastic asphalt increases concrete asphalt mixtures' durability and self-healing capacity [4, 5]. Another study revealed that HL added to stone mastic asphalt modified with steel slag as an aggregate substitution increases adhesion, stability, and water resistance [6]. However, research on HL modification with steel slag stone mastic asphalt is limited; previous studies [6] have not examined the TPB test or analyzed fracture and displacement. The unresolved issue is how the effect of adding HL on the fracture and displacement of SMASS modified HL. This analysis is important because, in other studies, it has been revealed that the HL on mastic asphalt affect a significant loss of ductility and toughness with an increase in HL dosage, a stiffness effect evidenced by a rise in peak load, a reduction in failure deformation, and a decrease in total fracture-specific work, indicating a loss of fracture energy [7]. The findings contradict the positive impact presented earlier [1, 2, 6]. The research began in 2023 [6], and adding hydrated lime to steel slag stone mastic asphalt (SSMA) increased its adhesion between asphalt and steel slag aggregate. Besides, steel slag stone mastic asphalt can enhance self-healing through heat induction. The ability of steel slag to conduct in stone mastic asphalt mixtures causes the self-healing temperature threshold to be reached more quickly. Under this condition, the viscosity of the asphalt in the mix decreases, allowing the microcrack recovery process to occur. The problem is that the viscosity will increase with the addition of HL. The self-healing process will be challenging to achieve, and the purpose of steel slag in speeding up the self-healing process in the mixture will become useless due to improper HL dosage.

In the research above, it is suspected that optimal limits must be considered, depending on the other materials that form the mixture. Adding HL is suspected to increase adhesion, stability, and water resistance, but to a certain extent, because more than that will affect other performance, such as ductility, fracture displacement, and self-healing.

Self-healing with the heat induction method requires temperature regulation to achieve optimal capacity. It follows paper [5], self-healing in asphalt can begin at a temperature of 55 °C. The study [8, 9] confirms that the optimum self-healing asphalt temperature is slightly above the softening point. Concrete asphalt that has undergone pre-cracking can be cured at a temperature ranging from 70 °C to 120 °C [10, 11] with a performance above 100 % at this temperature. In paper [5], the maximum healing performance was at 90 °C. Baowe confirmed that self-healing occurred above the softening point [4, 9], and 90 °C was the maximum temperature without overheating. The mix design of asphalt concrete and the heating methods were used in this study vary. In the study [10, 11], porous asphalt concrete combined with steel wool fiber with the induction method, in the study [9], hot mix asphalt and substitution of steel slag, adding steel wool fiber, and using microwave. The sample in [4] consists of AC-13 variations with steel and iron slag, and is heated in a microwave. However, all studies provide evidence that incorporating conductive materials in metal fiber and metallic waste aggregate can increase heating speed in the self-healing process, particularly within the 70 °C to 90 °C range. More specifically, the optimal heating temperature for self-healing varies depending on the proportion and type of mix. Research on steel slag as a substitution material shows an optimal heating temperature of  $\pm 85$  °C [12]. Furthermore, a heating temperature of 85 °C on steel fiber-modified concrete asphalt results in an optimal healing rate [13, 14]. On the other hand, the average temperature in Indonesia has been 27 °C, with a maximum recorded temperature of 35.8 °C. The air temperature will affect the surface temperature of the asphalt pavement. Pavement surface temperature can reach 55 °C to 65 °C, while the air temperature is 27–35.8 °C. The findings and facts provide an opportunity to investigate the self-healing ability in tropical conditions because, with high air temperature, artificial heating does not require significant energy to reach the threshold healing condition. The laboratory self-healing test so far has been using room temperature. This study uses induction heating designed for tropical ambient temperatures to apply self-healing technology and evaluate its effectiveness in tropical areas.

All the above concepts demonstrate the potential use of steel slag in stone mastic asphalt-modified HL to improve self-healing under tropical conditions. Research on self-healing performance in a mixture of steel slag stone mastic asphalt, with modified HL under tropical conditions, has not been carried out until now. This challenge is to get the right proportions so that adding HL increases fracture force but does not decrease its self-healing capacity. In this study, the cracking resistance index and flexibility index were also tested to assess the impact of HL on mixed cracking resistance.

Based on the research above, all studies are still at the stage where HL is used to mix with asphalt mastic or stone mastic asphalt and to analyze their properties. Laboratory research on self-healing in asphalt concrete mixtures is conducted at room temperature. However, previous studies have not examined the impact of HL on the self-healing properties of steel slag stone mastic asphalt for application in tropical temperatures. Therefore, this study was conducted to understand the application of the HL effect on steel slag stone mastic mixtures with induction healing in tropical areas, to improve the durability and service life.

### 3. The aim and objectives of the study

The study aims to evaluate the effect of hydrated lime on the self-healing properties of steel slag stone mastic asphalt under tropical conditions, using an induction heating method. It is intended that the findings will clarify the self-healing phenomenon in stone mastic asphalt with HL modification and its potential for use in tropical regions. This will allow the application of artificial self-healing without special treatment or adding external heating, but will be sufficient with natural heating. However, effectiveness will still be compared to artificial heating.

To achieve this aim, the following objectives are accomplished:

- analyze the effect of hydrated lime on steel slag stone mastic asphalt fracture;
- analyze the effect of hydrated lime on steel slag stone mastic asphalt refracture and healing index in natural and booster temperature conditions;
- analyze the effect of hydrated lime on the cracking resistance and flexibility index of steel slag stone mastic asphalt in natural and booster temperature conditions.

### 4. Materials and methods

#### 4.1. Object and hypothesis of the study

The object of study is modified steel slag stone mastic asphalt incorporating a variation of hydrated lime (HL) and exhibiting a high self-healing capacity. Its application in tropical climatic conditions evaluated. The mixture combines stone mastic asphalt with steel slag and includes hydrated lime. The compacted mixtures are subjected to a three-point bending test. Following this, the fracture beams undergo a healing process via induction heating, after which the three-point bending test is repeated on the healed specimens. The main hypothesis of this research is that the hydrated lime (HL) level will affect fracture and refracture, self-healing capacity, and cracking resistance.

This study assumes that heating with an induction engine, which is regulated to the surface temperature of the specimen according to the temperature reached in the field, represents a natural heating condition. The added temperature of the induction machine that the surface temperature reaches 85 °C for 2 minutes assumed to be artificial heating on the field.

#### 4.2. Material, specimen preparation

The materials used in the study are described as follows;

Basalt aggregate from Pasuruan, Indonesia, has a particle size distribution presented in Fig. 1. The binder requirements involve 60/70 penetration asphalt. The steel slag aggregate provided by Krakatau Steel Indonesia company serves as a substitute aggregate at 60 % for the size

range from 4.75 to 9.5 mm. Additionally, 0.3 % cellulose bamboo fiber is included in the mix for stabilization. Powdered hydrated lime was incorporated in various proportions, ranging from 1 % to 4 % by weight of the mixture. The chemical compounds of hydrated lime are detailed in Table 1.

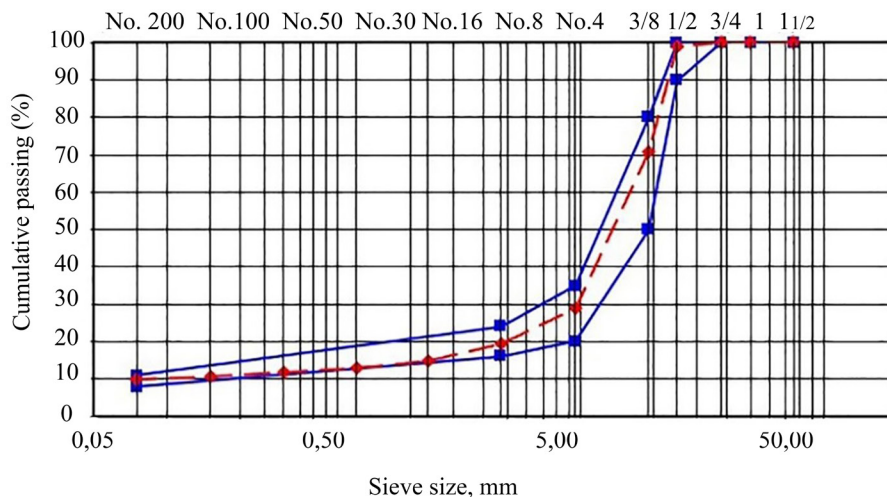


Fig. 1. Particle size distribution of aggregate

Steel slag stone mastic asphalt without hydrated lime was used as a control specimen, labeled SMASS, while SMASS modified with hydrated lime is labeled as SMASS1, SMASS2, SMASS3, and SMASS4. Details of the physical proportions of the mix are presented in Table 2.

Table 1

Chemical compounds of hydrated lime

Compounds	Concentration (%)
Ca	95
HCl	0.05
Cl	0.01
SO <sub>4</sub>	0.2
Fe	0.01
Pb	0.002
MgO	0.5
NH <sub>4</sub> OH	0.25

Table 2

The mixture proportion of different variant specimens

Specimen ID	Aggregate	Steel-slag	Asphalt %	Cellulose %	Hydrated lime (%)	Air void
SMASS	Basalt	60 % at size particle 4.75–9.5 mm	6.5	0.3	0	5
SMASS1	Basalt				1	4
SMASS2	Basalt				2	4
SMASS3	Basalt				3	4
SMASS4	Basalt				4	4

The specimen mixing in this research follows the wet method, in which HL is blended with asphalt binder first, and then aggregate and steel slag are incorporated into the mixture. This method improves adhesion between aggregate, steel slag, and mastic [3].

The specimen for the three-point bending test was prepared by mixing modified stone mastic asphalt in a 400×450×80 mm mold (Fig. 2, a). Next, the specimen was



compacted to achieve the targeted air void content. Finally, the compacted slab was cut to dimensions of 380×50×63 (height) mm following the ASTM-10 test standard (Fig. 2, b).



Fig. 2. Preparation TPB test:  
a – slab specimens; b – beam specimens

The specimen is compacted using a plate compactor, requiring 60 passes to achieve the desired void target. The top and bottom of the mold must be covered with paper before compacting, as this specimen contains a high level of asphalt that can easily adhere to the mold. The slab was allowed to cool before being removed from the mold. After conditioning at room temperature for two days, it was cut into beam dimensions.

#### 4. 3. Flowchart of the study and method

The research process illustrated in Fig. 3 begins with preparing specimens SMASS, SMASS1, SMASS2, SMASS3, and SMASS4. The fracture of stone mastic asphalt was evaluated using the three-point bending test. The next step is to use induction heating to heal the damaged specimen and conduct TPB again.

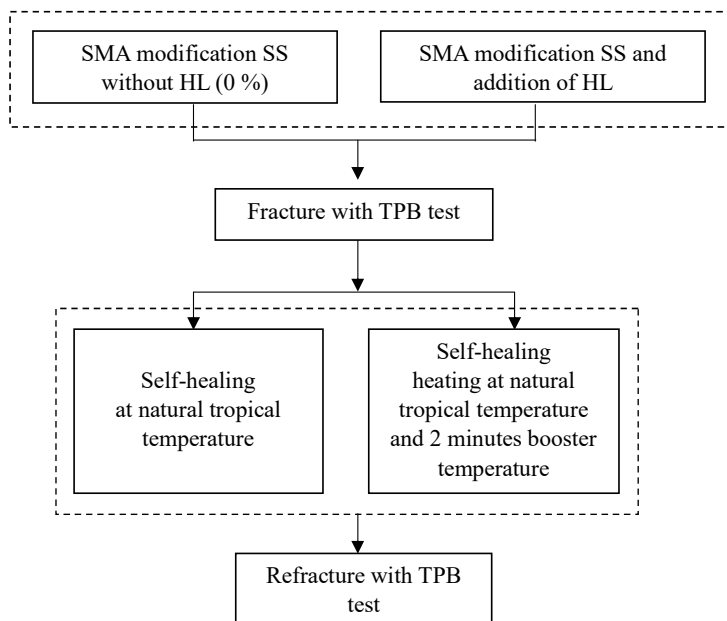


Fig. 3. Flowchart of the experiment

The self-healing system was studied under two conditions: at natural tropical temperatures, both with and without a temperature booster. In this case, temperature boosters were used to evaluate the effectiveness of induction machines as a means of artificial self-healing in tropical conditions. The following method for performing the tests will be discussed in detail.

#### 4. 4. Three-point bending test

The three-point bending (TPB) test is a commonly used laboratory procedure for determining the bending tensile strength of asphalt concrete. Fig. 4 illustrates the experimental setup for a TPB test, as per the ASTM D7460-10 standard.

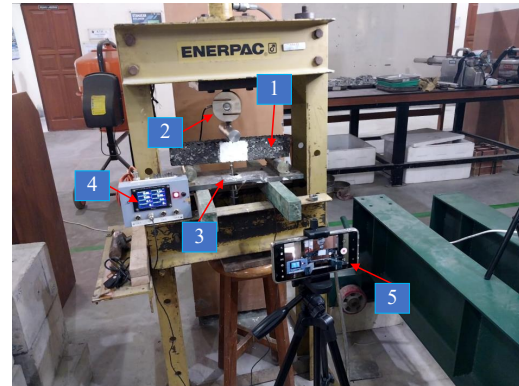


Fig. 4. The three-point bending test setup: 1 – specimen; 2 – load cell; 3 – LVDT; 4 – logger data; 5 – video recorder

The beams have been prepared with dimensions of 380×50×63 mm and loaded onto two pedestals with a span diameter of 250 mm. The load is applied continuously until damage occurs. Mid-span displacement was measured using the Linear Variable Differential Transducer (LVDT). During the TPB test, both displacement and beam loading changes are recorded. Damaged beams are placed in a flat plane and subjected to self-healing and refracture treatment through a repeat point-bending test. The three-point bending test is conducted before and after the damage-healing process at room temperature (25 °C).

#### 4. 5. Induction heating method

After TPB, the specimens underwent a healing process using induction heating. Induction heating is one of the artificial self-healing methods, which involves heating a surface specimen to a temperature above the softening point. Fig. 5 presents an experimental setup for induction heating. The machine includes a heating coil connected to a module that automatically regulates the desired temperature fluctuations.

An infrared camera and a thermometer gun monitor the temperature during heating. The induction machine utilized in this study has a capacity of 4 kW and a frequency of 50 Hz. The coil is positioned 8 cm from the specimen surface.

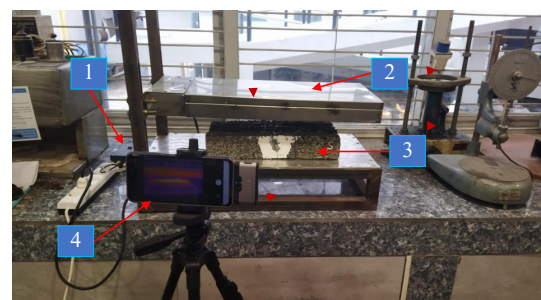


Fig. 5. The induction heating setup machine:  
1 – module; 2 – coil; 3 – specimen;  
4 – Infra-red camera

#### 4. 6. Temperature setting and healing process

This research simulated the temperature in field conditions and compared it with an increase to 85 °C on a surface specimen. In tropical countries such as Indonesia, the sun shines year-round, which supports natural self-healing. Only a small amount of additional energy is required to raise the temperature toward the target self-healing threshold.

The induction machine's effective heating period is calibrated to mimic tropical natural conditions for five hours, based on field measurements of the pavement surface. The effective heating period to achieve the healing temperature threshold is between 10:00 am and 3:00 pm. The average surface pavement used in the research is based on observations made in October 2024 of the field surface of the asphalt concrete wearing course (AC-WC). From this data, the machine is set to create a surface temperature of AC-WC pavement as shown in Table 3. Furthermore, the machine adjusted to the temperature is used to heat modified stone mastic asphalt specimens.

Table 3

Temperature surface setting for natural condition heating on asphalt concrete

Time	Temperature (°C)
1	52
2	63
3	65
4	63
5	58

The research is conducted under two heating system conditions: heating at natural temperature and providing additional heating until the surface temperature reaches 85 °C within two minutes of natural heating durations. The addition of heating is intended to facilitate the implementation of artificial heating in the field. The target of 85 °C for 2 minutes on the specimen's surface temperature was selected based on earlier research [14] to achieve optimal self-healing. Self-healing capacity in the two conditions will be compared to understand the effectiveness of self-healing without and with the addition of heat or artificial induction in tropical climate conditions. The healing system in this study consists of three steps: heating, cooling, and curing for 5 hours each. The total healing period lasts over 15 hours. Fig. 6 explains the healing system applied in this research. The rest period in the field is the condition under which the pavement needs to recover by stopping the traffic load.

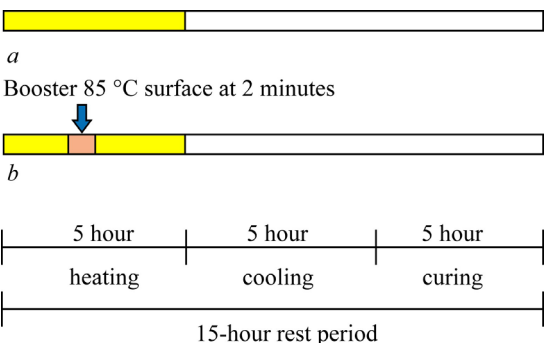


Fig. 6. Various healing systems in tropical temperatures:  
a – heating at natural temperature;  
b – heating with artificial temperature

After the 15-hour rest period of the specimen in the laboratory, the TPB test is repeated to obtain the remaining refracture force value following damage and healing.

#### 5. Result of hydrated lime's impact on the self-healing capacity of steel slag stone mastic asphalt

##### 5. 1. The effect of hydrated lime on steel slag stone mastic asphalt fracture

Applying the TPB test, specimens with five levels of hydrated lime are evaluated for fracture load and displacement. Fig. 7 illustrates a sample set of test results in a fracture force versus displacement graph. The Fig. 7 shows a tendency for the fracture force to increase as the hydrated lime content rises, while the displacement decreases. Fig. 8 presents the load versus displacement curve along with the parameters  $P_{max}$ ,  $l_{75}$ , and  $m_{75}$ . These parameters reflect the behavior of the asphalt mixture under stress. Here,  $l_{75}$  is the displacement length at which the load has decreased to 75 % of the peak load. The data were processed to obtain the average maximum fracture force ( $P_{max}$ ) and the 75 % post-peak load displacement ( $l_{75}$ ). The results of the maximum peak load rate from all TPB tests are displayed in Fig. 9.

The results of the TPB test on five specimen variants, each consisting of six test specimens, showed an increasing trend in the fracture force value with each addition of hydrated lime. Fig. 10 displays a graph of the displacement rate of the 75 % peak load in the post-peak area (mm) for each variant. This parameter indicates the deformation tolerance measured at 75 % of the peak load.

Fig. 7 illustrates how displacement behaves on the mixture. Compared to the SMASS modification with a higher HL level, the 1 % HL modification shows a displacement almost equal to the SMASS displacement.

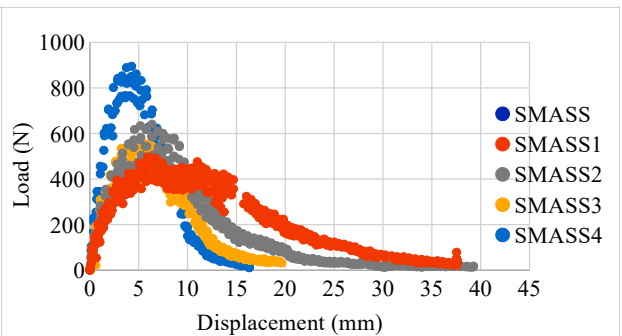


Fig. 7. Fracture force vs displacement curve pattern of the mixtures

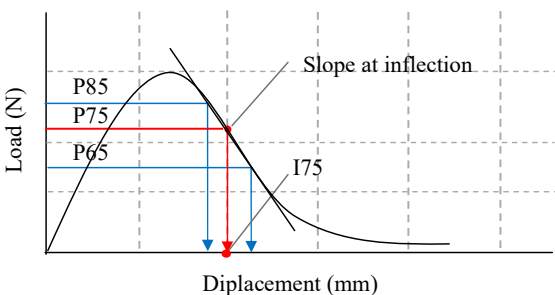


Fig. 8. Schematic of the total work of fracture in load vs displacement with  $P_{max}$ ,  $P_{75}$ ,  $l_{75}$ , and  $m_{75}$  values

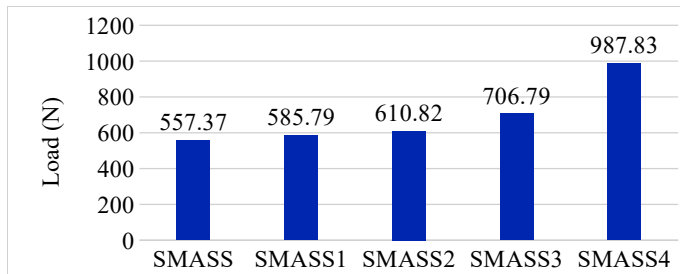


Fig. 9. Average maximum fracture force of the mixtures

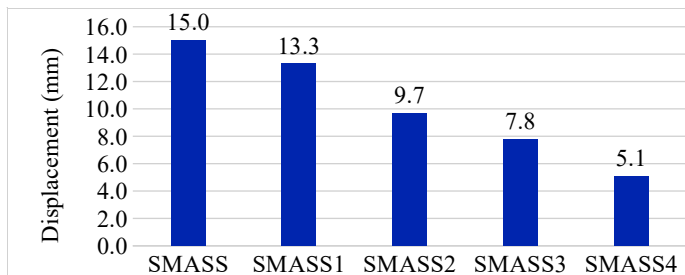
Fig. 10. Average displacement of 75 % post-peak load ( $l_{75}$ ) of the mixtures

Fig. 9 provides essential information about the fracture toughness of the SMASS mixture modified with HL. The 1 % HL modification increases fracture force by 5.1 % compared to the SMASS control at HL 0 % (from 557.37 N to 585.79 N). The 2 %, 3 %, and 4 % HL levels increased fractures by 9.5 %, 26.8 %, and 77.2 % compared to SMASS.

Fig. 10 presents a 75 % displacement post-peak load ( $l_{75}$ ).  $l_{75}$  measures 15.0 mm for SMASS and 13 mm for SMASS1, indicating a reduction of 11.33 %. Displacement at other HL levels shows significant reductions of 35.3 %, 48.2 %, and 66 % for HL 2 %, 3 %, and 4 %. There appears to be an increasing trend in peak load with higher HL dosage. As HL levels are added, the peak fracture force increases, while the displacement length decreases, as illustrated in Fig. 7, 9, 10.

## 5. 2. The effect of hydrated lime on steel slag stone mastic asphalt on healing performance with natural and booster temperature conditions

### 5. 2. 1. Thermal distribution, refracture, and healing process

Specimens that cracked during the TPB test underwent a self-healing treatment using the heat induction method at natural tropical temperatures. The results of the surface temperature observations are presented in Fig. 11.

The graph shows that the steel slag substitution in the mix increases the surface temperature of the specimen. Compared to the surface temperature of the AC-WC mixture used to determine the engine temperature (Table 3), the average temperature increases by 9.94 %. It is demonstrated that the substitution of steel slag increases the surface temperature of the mixture. Adding HL to SMASS indicated a decreased pattern at the surface temperature.

Specimens treated with a surface temperature increase of 85 °C for 2 minutes show a pattern of surface temperature rate increase as shown in Fig. 12. Booster heating at the 3<sup>rd</sup> hour causes the average surface temperature to increase in one hour to 67 °C–80 °C. Compared to heating at natural temperatures, there is an average hourly temperature increase of  $\pm 5$  %.

After the damaged process is carried out by heating induction on the specimens, the specimens are grouped into two groups. Group 1 was tested by heating at natural temperature, and group 2 was tested with additional heating until it reached a surface temperature of 85 °C for 2 minutes.

After the cooling and curing time, followed by a total 15-hour healing period, the TPB test is repeated to obtain a refracture force. Fig. 12 shows the pattern of the refracture vs displacement mixtures using the natural temperature heating method. The chart pattern shows that the refracture force and the displacement value tend to decrease as HL is added, except for the HL variation of 1 %. In the HL variation of 1 %, the refracture force value tends to be higher, but with a displacement length that is almost the same as the mix with HL 0 % (SMASS).

Fig. 13 shows a graph of refracture vs. displacement with healing at natural temperature and an increase of 85 °C for 2 minutes. The chart pattern shows that the refracture force and displacement tend to decrease with adding HL, except for adding 1 % HL. The refracture force and displacement have a similar pattern to SMASS without HL (HL 0 %).

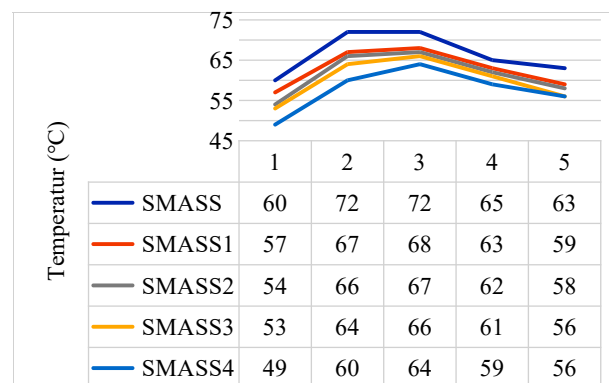


Fig. 11. Surface temperature on specimens under natural conditions

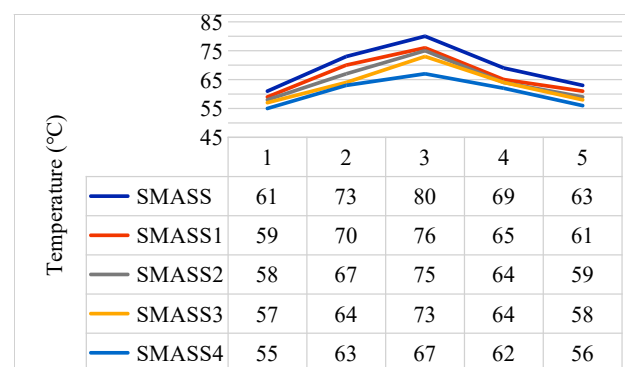


Fig. 12. Surface temperature on specimens with artificial conditions

Fig. 13, 14 indicate that after healing, the refracture and displacement patterns of SMASS and SMASS1 are not much different. Meanwhile, the SMASS curve pattern with an additional HL of more than 1 % shows much lower refracture force and displacement values. The shape of the curve becomes shorter and shifts to the left. This indicates that the

mixture with HL above 1 % has a low self-healing capacity, compared to SMASS and SMASS1.

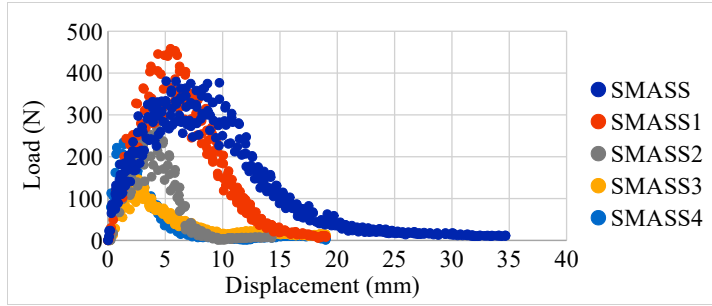


Fig. 13. Refracture force of SMASS in natural heating

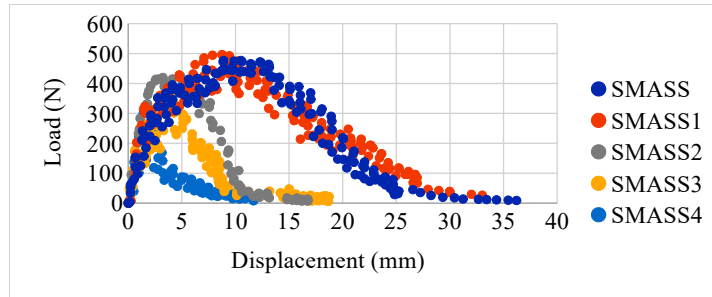


Fig. 14. Refracture force of SMASS in artificial heating temperature

The self-healing capacity of modified stone asphalt mixtures was assessed by comparing fracture strength before and after healing. The formula used is like equation (1):

$$HR = \frac{P_{after}}{P_{before}} \times 100\%, \quad (1)$$

where HR is healing ratio (%),  $P_{after}$  is the maximum fracture force after the damage-healing cycle,  $P_{before}$  is the maximum fracture force before the damage-healing cycle.

Fig. 15 explains the effect of HL on the healing ratio, which shows a parabolic pattern with optimal values at 1 %. Fig. 15 also compares the healing ratio between the natural and booster temperature methods. The addition of 1 % HL showed an increased self-healing treatment with the natural heating and booster temperature methods. Adding HL 2 %, 3 %, and 4 % showed a decrease in healing capacity compared to the control mixture of SMASS. A comparison of healing capacity with natural heating and booster temperature showed that adding 85 °C heat for 2 minutes to the surface of the specimen increased the healing ratio, except for HL modification by 4 %.

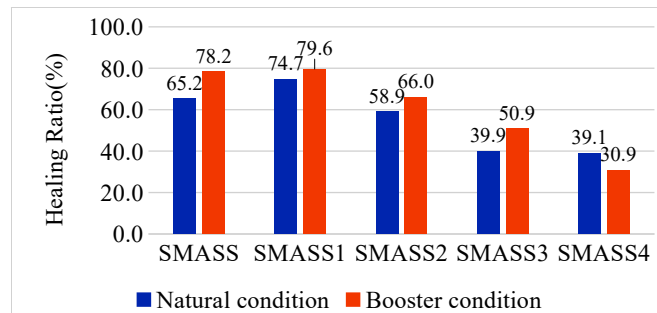


Fig. 15. Healing ratio of SMASS in natural heating and artificial heating/booster conditions

The difference in self-healing capacity with booster heating reached 4–13 % higher than natural heating, except for HL 4 %, where the self-healing capacity decreased with booster heating.

The healing ratio of HL 1 % modified stone mastic asphalt increased by 14.57 % under natural conditions compared to steel slag stone mastic asphalt. The healing ratio of steel slag mastic asphalt with artificial heating temperature rises by 22.08 %, compared with steel slag mastic asphalt with natural heating.

### 5.3. The effect of hydrated lime on steel slag stone mastic asphalt cracking resistance

#### 5.3.1. Cracking resistance index and flexibility index

The cracking resistance assessment is usually calculated by the cracking tolerance index (CT-Index). The resistance of asphalt mixtures to cracking is determined from the value of the CT index, mainly through the tensile cracking index test. CT index assessment is usually carried out with a cylindrical specimen with a diameter of 150 mm and a thickness of 62 mm. The same method to assess cracking is evaluated from the load vs displacement curve of the TPB test result in the form of a beam. The load vs displacement chart illustrates the area under the curve, which represents the energy ( $Wf$ ) required to crack the material. Therefore, a larger area under the curve indicates that the material is more capable of withstanding the appearance of a crack. The ability of the mixtures to reach more displacement or a higher peak load depends on how flexible the mixture is.

This study evaluated cracking by assessing the cracking resistance index (CRI). The CRI was introduced to address the limitations of existing performance metrics [18]. It was developed to differentiate between asphalt mixtures that exhibit similar  $Gf$  values but different peak loads ( $P_{max}$ ). The formula is expressed in (2), (3):

$$Gf = \frac{Wf}{A} = \frac{\int P du}{A}, \quad (2)$$

$$CRI = Gf / |P_{max}|. \quad (3)$$

Here,  $Gf$  is fracture energy ( $J/m^2$ ),  $Wf$  refers to the work of fracture ( $J$ ),  $P$  is applied load ( $N$ ),  $u$  is the load-line displacement LLD ( $m$ ),  $A$  is the ligament area ( $m$ ),  $CRI$  is the Cracking resistance index,  $P_{max}$  is peak load ( $N$ ).

As illustrated in Fig. 8, all the research data are evaluated based on cracking and flexibility performance. Cracking resistance, determined by integral values, relies on the area under the curve ( $\int P du$ ) divided by  $A$ , the specimen area subjected to loading, and the value of  $P_{max}$ . The results of the CRI calculation for the specimen before the healing process are presented in Fig. 16. From Fig. 16, it can be concluded that adding HL tends to reduce crack resistance. However, the difference in CRI value between SMASS and SMASS1 is minimal compared to SMASS2, SMASS3, and SMASS4. Meanwhile, the CRI values at other HL levels vary significantly from SMASS. Adding 1 % HL to SMASS led to a decrease in CRI of 2.6 %, and more significant additions of HL-2 %, 3 %, and 4 % resulted in reductions of CRI of 28.68 %, 40.89 %, and 43.08 %, respectively.



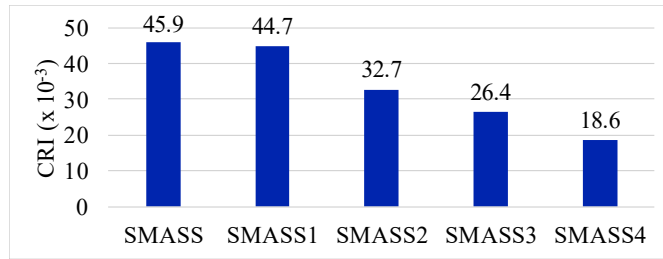


Fig. 16. Cracking resistance index (CRI) before the damage-healing process

The flexibility index (FI) is a performance indicator used to evaluate the cracking resistance of asphalt mixtures. This index demonstrated effectiveness in distinguishing the cracking resistance among various asphalt mixtures. The formula is expressed in (4), (5):

$$FI = \frac{Gf}{|m75|} \times 0.01, \quad (4)$$

$$|m75| = \left| \frac{P_{85} - P_{65}}{l_{85} - l_{65}} \right|, \quad (5)$$

where  $FI$  is flexibility index,  $m_{75}$  is the slope at 75 % of the peak load,  $P_{85}$  is the load at 85 % of the peak load (N), and  $P_{65}$  is the load at 65 % of the peak load (N).

The slope ( $m$ ) at the inflection point is a critical parameter that captures the rate at which the material loses its load-bearing capacity after the peak load. A gentler slope indicates more ductile behavior, which is associated with better cracking resistance. Fig. 17 illustrates the result of the FI calculation on the specimen before the healing process

Fig. 17 shows that adding 1 % HL resulted in a 22.38 % decrease in the flexibility index (FI). Increasing HL to 2 %, 3 %, and 4 % caused an even more significant average reduction in FI of 62 %. This suggests that the flexibility index decreases with the HL addition, with a more substantial decline occurring at levels above 1 % HL.

After the specimen underwent damage healing at natural and booster temperatures, its cracking resistance and flexibility were assessed. The maximum refracture pattern remains consistent with the fracture before healing. However, a slight difference exists in the artificial heating method, where the refracture value at 1 % HL (SMASS1) matches the value at 0 % HL (SMASS).

The crack resistance index (CRI) assessment after the damage-healing cycle process showed that the addition of HL to SMASS was reduced with natural heating treatment, as the CRI value was below the temperature booster. The behavior of SMASS modified HL after self-healing showed there was a consecutive decrease of CRI of 26 %, 53 %, 70 %, and 79 % in SMASS1, SMASS2, SMASS3, and SMASS4 compared to SMASS (0 % HL) under natural heating. In the booster heating, SMASS modified HL after self-healing showed a consecutive decrease of CRI of 48 %, 59 %, and 77 %, in SMASS2, SMASS3, and SMASS4, compared to SMASS (0 % HL). Specimens with booster heating treatment exhibited the same

CRI values in SMASS and SMASS1. In contrast, values decreased in SMASS2, SMASS3, and SMASS4 (Fig.18). A comparison of the CRI of the two conditions is presented in Fig. 18. Comparing the two methods reveals that increasing the temperature to 85 °C for 2 minutes on the surface of specimens generally produces a higher CRI across all HL levels. The average CRI increase was 17.7 % in SMASS, SMASS1, SMASS2, SMASS3, and SMASS4; however, in SMASS1, there was a decrease of 1.7 % (Fig. 18).

An evaluation of the mixture's flexibility (FI) was conducted following the damage-healing process, with results shown in Fig. 19. Based on the data, it can be concluded that the addition of HL to SMASS generally decreases flexibility, particularly with increments greater than 1 %. The behavior of SMASS modified HL after self-healing showed there was a consecutive decrease of FI of 22 %, 76 %, 93 %, and 94 % in SMASS1, SMASS2, SMASS3, and SMASS4 compared to SMASS (0 % HL) under natural heating. In the booster heating, SMASS modified HL after self-healing showed a consecutive decrease of FI of 15 %, 77 %, 87 %, and 97 % in SMASS1, SMASS2, SMASS3, and SMASS4, compared to SMASS (0 % HL).

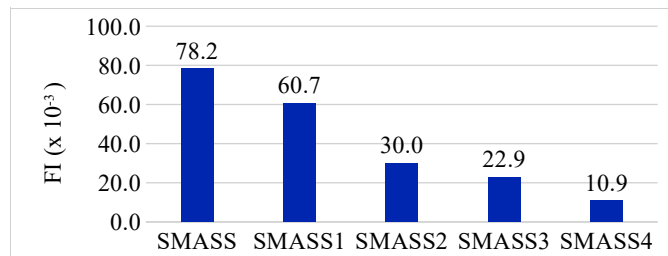


Fig. 17. Flexibility index (FI) of specimens before the damage-healing process

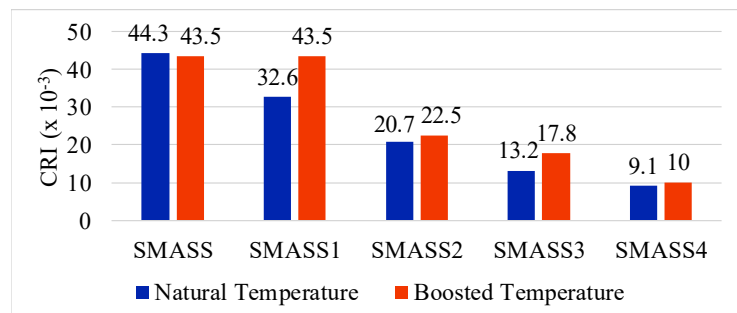


Fig. 18. Cracking resistance index of specimens after a damage-healing process

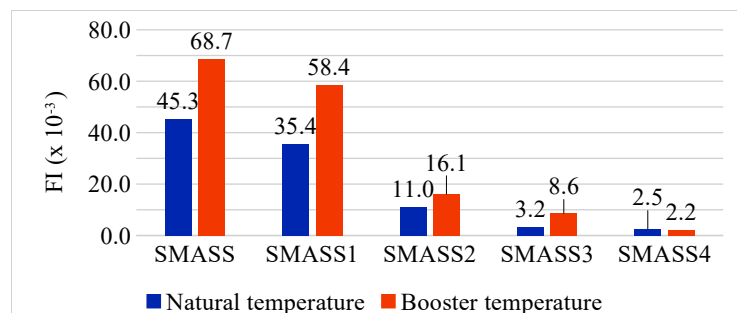


Fig. 19. Flexibility index of specimens after a damage-healing process



Fig. 19 also presents a comparative analysis of the flexibility index under natural conditions and at elevated temperatures. Heating to 85 °C from natural temperature resulted in an 82.2 % increase in the flexibility index rate.

FI value indicates the mixtures' flexibility, and the results suggest that HL addition reduces the FI value at all levels. SMASS and SMASS1 exhibited the best performance compared to FI at all HL levels.

## 6. Discussion of hydrated lime's effect on self-healing steel slag stone mastic asphalt with the induction heating method in tropical conditions

The research results prove that HL modification on steel slag stone mastic asphalt mixes significantly increases the fracture strength, but a decrease in displacement length follows. These results are consistent with earlier research [7], which reported that adding HL to the mastic asphalt increased peak load and decreased deformation. Research [7] on HL-modified asphalt mastic combining HL, limestone, and asphalt 30/45 reported an increase in fracture on the load-displacement curve. Those studies conclude that using a low HL concentration (6.7 % by weight of asphalt) minimizes the adverse impact on fracture performance. As more HL is added to the mastic, it reaches a higher peak load and lower displacement, indicating a stiffer mastic, representing a significant loss of ductility and a greater gain of strength. Compared to this research, composite mixtures of 60/70 asphalt and steel slag stone mastic asphalt are used; the results show that using 1 % HL by total weight of the mix or 15 % by asphalt provides a balance between stiffness and flexibility. Adding HL 2–4 % by weight of the mix or 30.7–61.7 % by weight of asphalt increases the peak load and failure deformation (Fig. 7, 9, 10). Adding HL of 1–2 % showed an increase in large fractures force (5.1 % and 9.5 %), but adding above 2 % showed a dramatic rise in fracture force of 26.6 % and 77.2 % (Fig. 9).

This study evaluated the mixtures' crack resistance. The HL effect led to an increase in the  $m_{75}$  value and a decrease in the CRI and flexibility index (FI) values (Fig. 16, 17). The decreasing CRI difference between SMASS (0 % HL) and SMASS1 (1 % HL) is 2.6 %. This value is the smallest compared to the percentage decreasing difference in CRI values SMASS2, SMASS3, and SMASS4 (Fig. 16). The same pattern is shown in the FI value, where the decrease in FI difference between SMASS and SMASS1 is the lowest value of 22.38 % (Fig. 17).

The assessment of the self-healing capacity of the mixture was conducted using two heating methods for comparison. In this research, the healing of cracks using the heat induction method, without booster temperature treatment, reflects the natural heating of a tropical environment. In contrast, heating with additional temperature mimics induction devices designed to accelerate the self-healing process. Observations of surface temperature using these two methods concluded that a tropical climate, with an average temperature of 27 °C and a maximum temperature of 31 °C, increased the surface temperature of the modified steel slag SMA and HL to 72 °C (Fig. 10). Meanwhile, applying heating for 2 minutes to achieve a surface temperature of 85 °C can elevate the average surface temperature over one hour to 80 °C (Fig. 11). Compared to a field survey that tested the temperature of AC-WC pavement with temperature gradations, as shown in

Table 3, the addition of steel slag to the SMA mix resulted in an increase in surface temperature by 8 % to 15 %. The addition of HL tends to lower the surface temperature of SMASS. The surface temperature of the mix affects the temperature threshold in healing conditions. However, overheating on the pavement surface can accelerate the aging process. The difference of 8 °C in peak surface temperatures between natural and artificial conditions has produced a higher healing ratio.

The self-healing capacity was assessed by comparing the peak load fracture before and after healing. The healing ratio indicates that natural heating for a 15-hour healing period restores the mix with a capacity of 39 % to 75.5 %. Fig. 14 depicts the optimal condition of the self-healing mixture with 1 % HL as an additive. This 1 % HL results in a mix with the highest self-healing capacity of 75.3 % compared to other HL-level modified specimens. This aligns with previous research, which explains that the addition of steel slag as a substitute material reduces the cohesion force between aggregate and asphalt, but incorporating 1–2 % HL increases cohesion [6]. The increased cohesion in this case enhances the self-healing abilities. The self-healing capacity of the mixture, with an additional heating of 85 °C for 2 minutes, ranges from 33.3 % to 78.8 %. Under natural heating, there was a 10 % increase in the self-healing capacity of SMASS1(HL 1 %) compared to SMASS specimens, while the self-healing capacity of other HL levels decreased.

Compared to the natural heating method, the booster temperature in the healing method for SMASS-modified HL induces an increase in the healing ratio at all HL levels (Fig. 15). In the booster method with a surface temperature of 85 °C maintained for 2 minutes, there was only a 0.5 % increase in self-healing capacity for SMASS1 compared to SMASS. Adding 1 % HL enhances the self-healing capacity of both heating methods.

The load versus displacement graph (Fig. 7) illustrates the HL effects on the SMASS; the load peak increases with additional HL while displacement decreases. The stiffening effect on the mix is evident, as shown by the curve's behavior. However, after the damage healing process at natural and artificial temperatures, the curve displays a different pattern (Fig. 13, 14), showing a decrease in peak load and less displacement with rising HL levels. The area under the curve also diminishes, indicating that the material loses ductility and strength after damage-healing, except for the mix with 1 % HL. The pattern of refracture vs displacement of SMASS 0 % HL is not much different from SMASS 1 % HL.

An assessment of CRI and FI values after self-healing corroborated the suggestion that they tended to decrease with adding HL (Fig. 18, 19). However, there was an increase in self-healing capacity with 1 % HL (SMASS1), regardless of external treatment. This demonstrates that SMASS with 1 % HL can enhance road service life.

The research findings demonstrated that 1 % HL modified steel slag stone mastic asphalt can be used in tropical conditions, allowing for a 15-hour healing rest period without artificial heating (Fig. 15). This results in a 14.57 % increase in self-healing capacity. Applying artificial heating to the mixture will further enhance the self-healing capacity by 22.08 % compared to SMASS (HL=0 %).

This study's limitation is that the method of measuring fracture strength is carried out only with a three-point bending test; other methods must be tested to validate the result. The study's shortcomings are that the temperature used to mimic the tropical environment is the temperature

of an area in the hottest month of the year; there needs to be more temperature variation. In addition, the rest period of the specimen in the test is 15 hours, which means that traffic must stop for 15 hours in the application. The closure of the road for recovery during this time is still too long in practice, and an innovation is needed to shorten the rest period.

The results can be utilized for further research by comparing samples of various hot-mix asphalt mixtures. This will allow the efficiency of the mixes' use to be measured based on their self-healing capacity.

7. Conclusions

1. Adding HL to SMASS revealed a stiffening effect, evidenced by increased peak loads and fracture, but reduced failure displacement. The 1 % HL modification increases fracture force by 5.1 %. The 2 %, 3 %, and 4 % HL levels increased fracture force by 9.5 %, 26.8 %, and 77.2 % compared to SMASS (HL=0 %). Displacement post-peak load 75 % (I75) indicates an 11.33 % reduction for the 1 % HL modification. Displacement at other HL levels shows significant decreases of 35.5 %, 48.2 %, and 66 % for HL 2 %, 3 %, and 4 %.
2. Adding HL to the SMASS mixture decreases the refracture force after self-healing, except for 1 % HL. The healing performance under the natural tropical heating method achieved a healing ratio of 74.7 % at 1 % HL, declining with additions above 1 %. The artificial heating treatment in SMASS modified with 1 % HL demonstrated the highest healing ratio of 79.6 %. SMASS containing 1 % HL enhances self-healing performance under natural and artificial heating. The artificial heating treatment increases healing effectiveness by 4 % to 13 % compared to natural heating. The enhanced healing ratio under natural heating for the SMASS with 1 % HL reached 14.57 % compared to SMASS 0 % HL. The enhanced healing ratio under artificial heating of the SMASS 1 % HL reached 22.08 % compared to SMASS 0 % HL with natural heating.
3. The crack resistance of the mixture with the addition of HL, before and after the damage healing process, shows a downward trend in the CRI and Flexibility index (FI) values. The CRI assessment of SMASS1 (1 % HL) before self-healing revealed a decrease of 2.6 % and over 40 % for adding HL in

amounts greater than 2 %. The CRI assessment of SMASS1 after self-healing under natural conditions indicated a decrease of 26 % and more than 53 % for adding HL over 2 %. The CRI assessment of SMASS1 after self-healing with booster conditions showed the same CRI value as SMASS and a decrease exceeding 48% for adding HL in amounts greater than 2 %. The same pattern is reflected in the FI value, where the reduction in the FI difference between SMASS and SMASS1 presents the lowest value at 22.38 %. The FI value of SMASS1 after self-healing under tropical heating was 22 %, and 15 % under booster heating, compared to SMASS.

Conflict of interest

The authors declare that they have no conflict of interest with this research, whether financial, personal, authorship, or otherwise, that could affect the study and its results presented in this paper.

Financing

The study was performed without financial support.

Data availability

The manuscript has no associated data.

Use of artificial intelligence

The authors confirm they did not use artificial intelligence technologies when creating the current work.

Acknowledgments

The authors thank the research team members for their guidance and support throughout LPPM Brawijaya, LPPM Muhammadiyah Jember University, and Krakatau Steel Indonesia Company.

References

1. Diao, H., Ling, T., Zhang, Z., Peng, B., Huang, Q. (2023). Multiscale Fatigue Performance Evaluation of Hydrated Lime and Basalt Fiber Modified Asphalt Mixture. *Materials*, 16 (10), 3608. <https://doi.org/10.3390/ma16103608>
2. Movilla-Quesada, D., Raposeiras, A. C., Castro-Fresno, D., Peña-Mansilla, D. (2015). Experimental study on stiffness development of asphalt mixture containing cement and Ca(OH)2 as contribution filler. *Materials & Design*, 74, 157–163. <https://doi.org/10.1016/j.matdes.2015.02.026>
3. Carvajal-Muñoz, J. S., Airey, G., Sanjuan-Benavides, A., Perez-Miranda, M. A., Gómez-Osorio, F. A. (2024). Fracture characteristics of SMA mixtures with hydrated lime through the semi-circular bending approach. *Construction and Building Materials*, 449, 138353. <https://doi.org/10.1016/j.conbuildmat.2024.138353>
4. Liu, J., Wang, Z., Li, M., Wang, X., Wang, Z., Zhang, T. (2022). Microwave heating uniformity, road performance and internal void characteristics of steel slag asphalt mixtures. *Construction and Building Materials*, 353, 129155. <https://doi.org/10.1016/j.conbuildmat.2022.129155>
5. Phan, T. M., Park, D.-W., Le, T. H. M. (2018). Crack healing performance of hot mix asphalt containing steel slag by microwaves heating. *Construction and Building Materials*, 180, 503–511. <https://doi.org/10.1016/j.conbuildmat.2018.05.278>
6. Irawati, I., Djakfar, L., Arifin, M. Z. (2023). Comparison of the moisture resistance of a steel-slag stone mastic asphalt mixture modified with Ca(OH)2. *Eastern-European Journal of Enterprise Technologies*, 6 (6 (126)), 62–70. <https://doi.org/10.15587/1729-4061.2023.289054>

7. Carvajal-Muñoz, J. S., Airey, G., Hernández-De Las Salas, R. D., Contreras-Barbas, M. A., Rodríguez-Verdecia, S. A. (2024). Fundamental cracking performance of asphalt-filler mastics with hydrated lime. *Construction and Building Materials*, 453, 139029. <https://doi.org/10.1016/j.conbuildmat.2024.139029>
8. Xiang, H., He, Z., Chen, L., Zhu, H., Wang, Z. (2019). Key Factors and Optimal Conditions for Self-Healing of Bituminous Binder. *Journal of Materials in Civil Engineering*, 31 (9). [https://doi.org/10.1061/\(asce\)mt.1943-5533.0002760](https://doi.org/10.1061/(asce)mt.1943-5533.0002760)
9. Lou, B., Sha, A., Li, Y., Wang, W., Liu, Z., Jiang, W., Cui, X. (2020). Effect of metallic-waste aggregates on microwave self-healing performances of asphalt mixtures. *Construction and Building Materials*, 246, 118510. <https://doi.org/10.1016/j.conbuildmat.2020.118510>
10. Liu, Q., Schlangen, E., van de Ven, M. F. C., van Bochove, G., van Montfort, J. (2012). Predicting the Performance of the Induction Healing Porous Asphalt Test Section. 7th RILEM International Conference on Cracking in Pavements, 1081–1089. [https://doi.org/10.1007/978-94-007-4566-7\\_103](https://doi.org/10.1007/978-94-007-4566-7_103)
11. Liu, Q., Schlangen, E., van de Ven, M., van Bochove, G., van Montfort, J. (2012). Evaluation of the induction healing effect of porous asphalt concrete through four point bending fatigue test. *Construction and Building Materials*, 29, 403–409. <https://doi.org/10.1016/j.conbuildmat.2011.10.058>
12. Vila-Cortavitarte, M., Jato-Espino, D., Castro-Fresno, D., Calzada-Pérez, M. Á. (2018). Self-Healing Capacity of Asphalt Mixtures Including By-Products Both as Aggregates and Heating Inductors. *Materials*, 11 (5), 800. <https://doi.org/10.3390/ma11050800>
13. Li, H., Yu, J., Wu, S., Liu, Q., Li, Y., Wu, Y., Xu, H. (2019). Investigation of the Effect of Induction Heating on Asphalt Binder Aging in Steel Fibers Modified Asphalt Concrete. *Materials*, 12 (7), 1067. <https://doi.org/10.3390/ma12071067>
14. Kaseer, F., Yin, F., Arámbula-Mercado, E., Epps Martin, A., Daniel, J. S., Salari, S. (2018). Development of an index to evaluate the cracking potential of asphalt mixtures using the semi-circular bending test. *Construction and Building Materials*, 167, 286–298. <https://doi.org/10.1016/j.conbuildmat.2018.02.014>